Contrasting Impacts of the Indian Ocean Dipole and ENSO on the Tropospheric Biennial Oscillation

Toru Tamura[1], Toshio Koike[1], Akio Yamamoto[2], Masaki Yasukawa[2], and Masaru Kitsuregawa[2]
[1]*Department of Civil Engineering, The University of Tokyo, Tokyo, Japan*
[2]*Institute of Industrial Science, The University of Tokyo, Tokyo, Japan*

Abstract

There is a biennial tendency for the interannual variabilities of the Asian summer monsoon (ASM) referred to as the tropospheric biennial oscillation (TBO). Previous studies have emphasized that land–atmosphere–ocean interactions in association with the El Niño/Southern Oscillation (ENSO) and Indian Ocean Dipole (IOD) trigger a phase shift of the TBO from one year to another. However, simple lead-lag correlations among the ASM, IOD and ENSO indices reveal that there is a relatively stronger signal of the phase shift of the ASM over two years than one year. Meanwhile, the IOD has been shown to contribute to the TBO by triggering the phase shift of the ENSO by the following winter, although correlations of the ENSO do not identify such a biennial tendency. Through composite analyses, IOD–ENSO coupled events are shown to induce the phase shift of the ENSO within a year, which results in a distinctive TBO pattern of the ASM in the following two years. In contrast, ENSO events without the IOD cannot induce the phase shift, and there is no TBO pattern in the following two years. Thus, IOD–ENSO coupled events and independent ENSO events have contrasting roles in inducing different (two-year and four-year) frequencies of the ASM interannual variability in subsequent years.

1. Introduction

Large-scale sea surface temperature (SST) associated with the El Niño/Southern Oscillation (ENSO), has a strong influence on the Asian summer monsoon (ASM). The El Niño (La Niña) phase of the ENSO, which matures toward the boreal winter, usually leads to a stronger (weaker) ASM in the following season (e.g., Rasmusson and Carpenter 1983; Meehl 1987; Webster and Yang 1992; Ju and Slingo 1995; Kawamura 1998).

The interannual variabilities of the ASM have been identified to have a biennial tendency (e.g., Trenberth 1975) referred to as the tropospheric biennial oscillation (TBO). Since the atmospheric response to the external forcing by the ocean can last for a long time, the Pacific SST forcing in association with the ENSO has been emphasized as an important conductor of the TBO (Goswami 1995; Meehl and Arblaster 2001; Pillai and Mohankumar 2007). The basic concept of the TBO is based on large-scale atmosphere–ocean interactions in which a season with higher SST leads to greater convection and stronger winds that subsequently result in higher evaporation and lower SST in the following season (Meehl 1993; Goswami 1995). By advancing that concept, the TBO was proposed to be coupled land–atmosphere–ocean interactions in which the Asian–Australian monsoon plays an active role to induce the phase shift of the SST variability over the Indo–Pacific such as the ENSO (Meehl 1997; Ogasawara et al. 1999).

The Indian Ocean equivalent of the ENSO, i.e., the Indian Ocean Dipole (IOD; Saji et al. 1999), has been identified as another contributor of the interannual variability of the ASM (Webster et al. 1999; Ashok et al. 2001; Guan and Yamagata 2003; Yuan et al. 2008). During a positive IOD, anomalously low SSTs start to appear off Sumatra in summer, peaking in October through the Bjerknes feedback. The IOD has been suggested to be an important element of the TBO in which the coupled ASM–IOD system exerts retroactive feedback to maintain the biennial tendency by regulating meridional heat transport over the Indian Ocean associated with the variability of the monsoon westerly and its oceanic response (Loschnigg et al. 2003).

In a more recent study, the IOD was suggested to trigger the biennial phase shift of the ENSO (Izumo et al. 2010). The positive (negative) phase of the IOD in boreal autumn that simultaneously tends to co-occur with the El Niño (La Niña) phase of the ENSO (Annamalai et al. 2005; Sakai et al. 2010) was demonstrated to introduce the La Niña (El Niño) in the following year. The mechanism was suggested that the IOD modulates the Walker circulation even over the Pacific, and its oceanic response gives rise to the phase shift of the ENSO. Thus, the atmosphere–ocean interactions over the Indo–Pacific sector encouraged by the IOD seem to give the ENSO its biennial tendency, which in turn could be responsible for the biennial tendency of the ASM because of the close relation between the ENSO and the following ASM.

Thus, although most studies have investigated the mechanism of land–atmosphere–ocean interactions in association with the ENSO and IOD to trigger the phase shift of the TBO from one year to another, initial forcing of the SST is implied to have a long memory to influence atmospheric conditions in not only the next year but also the year after that. In this study, we investigate SST forcings of the IOD and the ENSO in terms of the following two-year variability of the ASM, and suggest they have contrasting roles in inducing different (two-year and four-year) frequencies of interannual variability.

2. Data and method

The meteorological data in this study are derived from the NCEP/NCAR reanalysis data (Kalnay et al. 1996). The SST data comes from the Hadley Centre Sea Ice and SST dataset (HadISST; Rayner et al. 2003), and precipitation data are obtained from the Global Precipitation Climatology Project (GPCP; Adler et al. 2003). We focused on the period from 1979 to 2008 when satellite derived data are available.

We used typical SST-based indices to present the ENSO and IOD cycles. The ENSO index is obtained from area-averaged SST anomalies over the Niño3 region (150°W−90°W, 5°S−5°N) during October–December. The IOD index is derived from the difference in SST anomalies between the western (50°E–70°E, 10°S–10°N) and eastern (90°E–110°E, 10°S–0°N) equatorial Indian Ocean during September–November.

We employed the monthly ASM intensity index based on the north–south gradient of upper-tropospheric thickness between the Asian continent and Indian Ocean, as proposed by Kawamura (1998). It is defined as the meridional difference in the area-averaged upper-tropospheric (500−200 hPa) thickness between the Tibetan Plateau region (50°E−100°E, 20°N−40°N) and the northern Indian Ocean (50°E−100°E, 0°N−20°N). That definition can be supported by studies as Xavier et al. (2007) which defined the ASM onset on the basis of difference in the upper-tropospheric (600−200 hPa) temperature and showed the interannual variability of the ASM onset is well represented by this thermal contrast. Thus, in order to evaluate not only the mature phase but also the

Corresponding author: Toru Tamura, The University of Tokyo, 7-3-1 Hongo Bunkyo-ku, Tokyo, Japan. E-mail: tamura@hydra.t.u-tokyo.ac.jp.

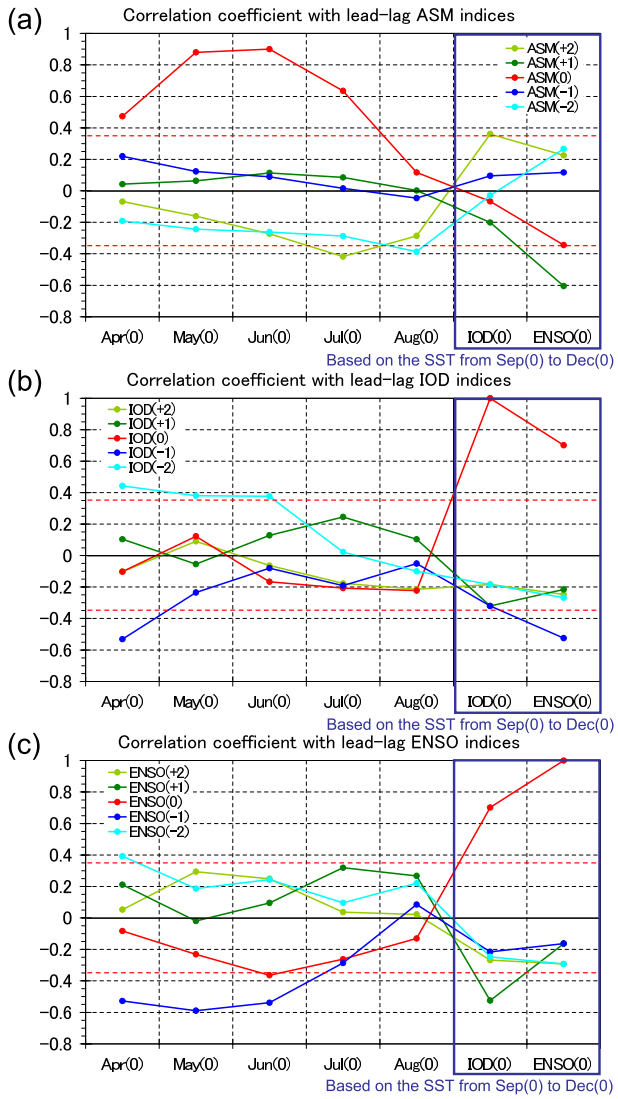

Fig. 1. Lead-lag correlation among the ASM, IOD and ENSO indices. (a) Correlation between the ASM, IOD and ENSO for a given year (spring to summer, fall and winter of year 0, respectively) and lead-lag ASM indices (average of May–July) in year-2 to year+2. (b) Same as (a), but for lead-lag IOD indices. (c) Same as (a), but for lead-lag ENSO indices. Red dashed lines indicate 5% significance levels.

onset phase of the ASM, we focused the variability of the ASM from May to July in this study.

3. Correlation analysis

To investigate how initial forcing of the SST is related to the biennial variability of the ASM, we conducted simple lead-lag correlation analyses among ENSO, IOD and ASM indices. Figure 1a shows the correlation coefficients between the lead-lag ASM indices (averaged from May to July) and monthly ASM as well as ENSO and IOD indices in a given year [indicated by (0)]. We can find there is no significant signal of biennial oscillation for the ASM [ASM(−1), ASM(+1)]. Instead, there is a relatively stronger signal of the phase change in two years [ASM(−2), ASM(+2)]. Correlation analysis for SST indices reveals precursory signals of the SST to the interannual variability of the ASM. The IOD is found to be less correlated with the preceding ASM [ASM(−2) to ASM(0)] than that following [ASM(+1), ASM(+2)]. It is noticeable that there is significant correlation between the IOD and the

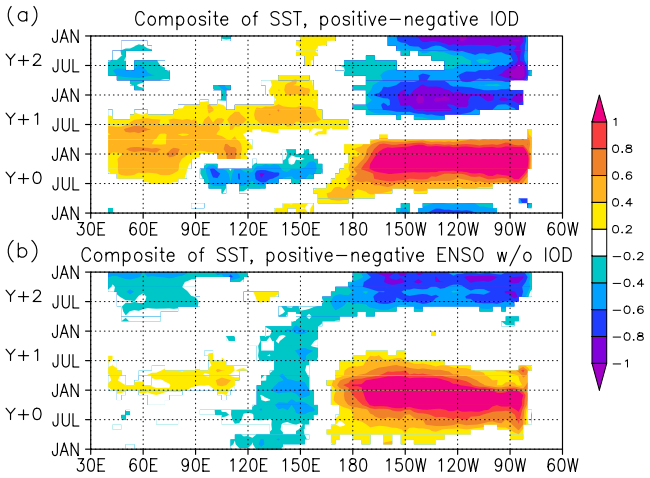

Fig. 2. Longitude-time cross section (10°S−10°N) of SST composites (unit: K) from January of year 0 to January of year+3. (a) Anomalous SST between positive and negative IOD years. (b) Anomalous SST between positive and negative ENSO years without the IOD. Values exceeding 5% significance level are shown.

ASM two years later.

More detailed correlation between the IOD and ASM is shown by Fig. 1b, which presents correlation coefficients for lead-lag IOD indices. It clearly confirms that the ASM in early summer is significantly and positively correlated with the IOD index two years before [IOD(−2)]. In addition, there is significant and negative correlation of the ASM in April with the IOD index one year before [IOD(−1)]. Thus, it is implied that the ASM has a biennial tendency if filtered by the IOD index. Meanwhile, the lead-lag correlation of the IOD with the ENSO confirms that the IOD not only tends to co-occur with the ENSO [IOD(0)] but also triggers a phase shift of the ENSO in the following year [IOD(−1)], as demonstrated by Izumo et al. (2010). Since the ENSO significantly affects the following ASM [Fig. 1a, ENSO(0) and ASM(+1)], the IOD-induced ENSO in the following year is implied to be responsible for the significant correlation between the ASM and the IOD two years before (Fig. 1b).

The lead-lag correlation of the ENSO is presented in Fig. 1c. It confirms that the ASM is significantly affected by the previous ENSO [ENSO(−1)] especially during early summer. However, there is no significant signal of biennial variability of the ASM [ENSO(−2)], which was confirmed against the IOD index (Fig. 1b). On the other hand, the influence of the ASM on the following ENSO [ENSO(0)] is found to be relatively weaker and insignificant. We also find that there is no significant correlation of the ENSO that clearly identifies an interannual cycle of the ENSO as shown by the lead-lag correlations among the ENSO indices.

4. Composite analysis

4.1 Phase shift of the ENSO

Lead-lag correlation analyses indicated that the IOD contributes to the TBO by triggering the phase change of the ENSO in the following year (Fig. 1b), although we cannot find a biennial tendency by projecting through the ENSO indices (Fig. 1c) and by simply lag correlating among the ASM indices (Fig. 1a). It is thus questionable why the biennial oscillation, as confirmed by power spectrum analysis (Meehl 1997; Ogasawara et al. 1999), could not be identified in Figs. 1a and c. Although the IOD tends to co-occur with the ENSO, the ENSO can develop even without the IOD. Here, to investigate the individual influences of the IOD and ENSO, we conducted composite analyses by defining positive/negative IOD and ENSO years.

We composed positive/negative IOD years based on the IOD index with more than one standard deviation. From 1979 to 2008,

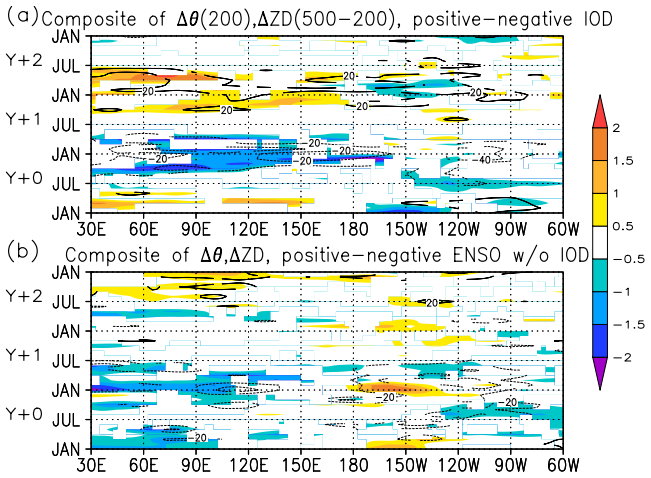

Fig. 3. Longitude-time cross section of the meridional difference (20°N−40°N minus 0°N−20°N) in the upper-tropospheric thickness (contour, unit: m) and 200 hPa potential temperature (color, unit: K). (a) Anomalies between positive and negative IOD years. (b) Anomalies between positive and negative ENSO years without the IOD. Values exceeding 10% significance level are shown.

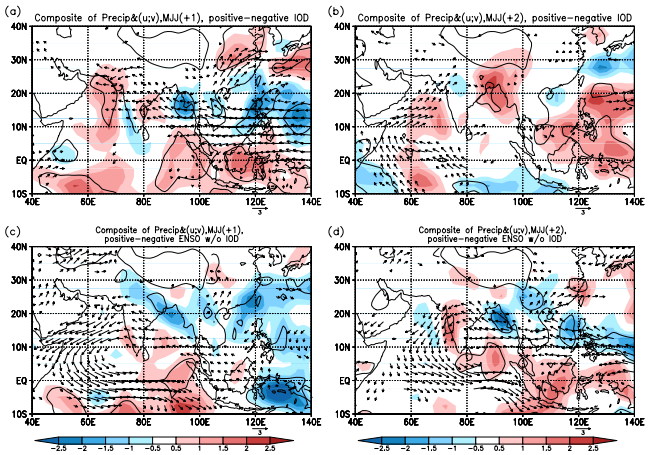

Fig. 4. Composites of precipitation (color, unit: mm day^{-1}) and wind vectors (unit: m s^{-1}) at 850 hPa averaged from May to July. (a) Anomalies between positive and negative IOD years in year+1. (b) Same as (a), but in year+2. (c) Anomalies between positive and negative ENSO years without the IOD in year+1. (d) Same as (c), but in year+2. Thin black contours are 10% significance level for precipitation and only wind vectors exceeding 10% significance level are shown. The thick black contour is the 3000 m altitude line indicating the Tibetan Plateau.

there are five positive IOD years (1982, 1994, 1997, 2002, 2006) and six negative IOD years (1980, 1981, 1984, 1992, 1996, 1998). In addition, we selected positive/negative ENSO years based on the ENSO index with more than half a standard deviation, but excluded IOD years. There are five positive ENSO years without the IOD (1979, 1986, 1987, 1991, 2003) and six negative ENSO years without the IOD (1988, 1995, 1999, 2000, 2005, 2007).

Figure 2 shows the longitude-time cross section of the equatorial SST (averaged from 10°S to 10°N). Figure 2a is for the difference in SST anomaly between the positive and negative IOD years. The positive phase of the IOD co-occurs with the El Niño during boreal autumn to winter (year 0). By the next winter (year+1), the IOD mode disappears and the El Niño is replaced by the La Niña. For the next year, there is no phase shift of the ENSO and the La Niña still dominates. Thus, there is the phase shift of the ENSO from one winter to another when there is the simultaneous IOD.

Figure 2b shows the difference in SST anomaly between the El Niño and La Niña years without the IOD. We can find that the El Niño that matures during the winter of year 0 still exists in the winter of year+1. The decaying El Niño during year+1 is subsequently replaced by the La Niña by the winter of year+2. The results in Figs. 2a and b reveal the crucial role of the IOD in triggering the phase shift of the ENSO within a year while the phase shift of the ENSO without the IOD takes mostly two years.

4.2 Contrasting impacts on the ASM

The contrasting impacts of the coupled IOD–ENSO and the independent ENSO on the following SST variability should result in contrasting interannual variability of the ASM. Figure 3 presents the longitude-time cross section of the meridional difference in the upper-tropospheric thickness, which is used for defining the ASM index (Section 2), and meridional difference in upper-level temperature at 200 hPa, which is above the reach of land surface heating even over the Tibetan Plateau (Tamura et al. 2010). Tamura and Koike (2010) demonstrated that the convective activity around the Maritime Continent plays an important role in inducing the seasonal evolution of the ASM as well as the upper-level warming around the Tibetan Plateau in early summer. Therefore, the local SST variability around the Maritime Continent associated with the ENSO is indicated to have the significant influence on the upper-level thermal contrast and the monsoon activity in the subsequent early summer.

Figure 3a is for the differences in the meridional gradients of thermal and tropospheric thickness between the positive and negative IOD years. From winter to early summer just after the occurrences of the positive IOD and ENSO, we can find reduced meridional upper-tropospheric thermal contrast over the ASM sector. On the other hand, there is enhanced thermal contrast in year+2 reflecting the La Niña during the preceding winter (Fig. 2a). Thus, there is a TBO pattern from year+1 to year+2, associated with the phase shift of the ENSO. Meanwhile, Figure 3b is for ENSO years without the IOD. The upper-tropospheric variability during year+1 is similar to that in Fig. 3a. However, in year+2, there is still reduced thermal contrast owing to the persisting El Niño (Fig. 2b).

To further confirm the contrasting impacts on the ASM, Figure 4 shows anomalies of the precipitation and wind field at 850 hPa averaged from May to July in year+1 and year+2. After the positive IOD event, the monsoon westerly and precipitation around the Southeast Asia are found to be suppressed (Fig. 4a) in accordance with the reduced thermal contrast (Fig. 3a). Then, the phase shift of the ENSO from the El Niño to La Niña in year+1 (Fig. 2a) leads to an enhanced ASM in year+2 (Fig. 4b). The ASM is also suppressed after the El Niño event without the IOD (Fig. 4c). However, the suppressed condition continues in year+2 (Fig. 4d) since the El Niño phase persists during the preceding winter (Fig. 2b).

Therefore, there is a distinctive TBO pattern in the following years after the IOD–ENSO coupled events that trigger the phase shift of the ENSO by the next winter. In contrast, the ENSO events without the IOD do not produce such a TBO pattern and take two years to trigger the phase shift of the ENSO and ASM. Such coexistence of different frequencies in the ENSO–ASM system must be a reason for the difficulty in finding TBO signals in the ASM and ENSO indices (Figs. 1a and c).

5. Summary

In this study, we investigated the role of SST forcings, i.e., IOD–ENSO coupled event and ENSO event without the IOD, on the interannual variability of the ASM in the following two years in association with the TBO.

Composite analysis based on the IOD and ENSO indices showed that the positive phase of the IOD which co-occurs with the El Niño during boreal autumn to winter (year 0) triggers the phase shift of the ENSO by the next winter (year+1), as shown by the previous study (Izumo et al. 2010). However, for the next year

without the IOD (year+2), there is no phase shift of the ENSO. Thus, the phase shift of the ENSO from one winter to another occurs when there is the simultaneous IOD. This is confirmed by the composite of the ENSO events without the IOD. The phase shift of the ENSO is not identified by the next winter (year+1) after the ENSO events without the IOD, but occurs by the winter of year+2. Consequently, the IOD plays a crucial role in triggering the phase shift of the ENSO within a year, whereas without the IOD, the phase shift of the ENSO is seen after two years.

Because of the phase shift of the ENSO within a year after the IOD–ENSO coupled events, there is a distinctive TBO pattern of the ASM in year+1 and year+2. In contrast, because there is no phase shift of the ENSO after ENSO events without the IOD, there is no TBO pattern but a consecutive stronger or weaker condition of the ASM in year+1 and year+2. Such contrasting impacts of SST forcings are considered to be the reason for the combined frequencies in the ENSO–ASM system; a two-year frequency (TBO) for the IOD–ENSO coupled events and four-year frequency for the independent ENSO events.

Even though we have focused on the IOD and ENSO, some of the studies emphasized the role of the basin-wide warming over the Indian Ocean, especially after the positive IOD–ENSO event (Fig. 2a), in inducing the interannual variability of the ASM (Tokinaga and Tanimoto 2004; Xie et al. 2009). However, SST anomaly after the negative IOD–ENSO event shows no significant SST cooling over the Indian Ocean even though it is followed by the phase shift of the ENSO (Fig. S1). We still need further investigations as numerical experiments to verify the roles of the IOD, ENSO and the basin wide warming over the Indian Ocean in the TBO.

Acknowledgements

The authors thank the editor and the anonymous reviewers for their comments that improved the original manuscript. This study is conducted under the frame work of the Data Integration and Analysis System (DIAS), which is one of five National Key Technologies defined by the 3rd Basic Program for Science and Technology of Japan.

Supplement

Figure S1 gives SST anomalies for positive (negative) IOD years as well as positive (negative) ENSO without IOD years, i.e., four cases, to show symmetric impacts of the IOD and ENSO.

References

Adler, R. F., G. J. Huffman, A. Chang, R. Ferraro, P.-P. Xie, J. Janowiak, B. Rudolf, U. Schneider, S. Curtis, D. Bolvin, A. Gruber, J. Susskind, P. Arkin, and E. Nelkin, 2003: The Version 2 Global Precipitation Climatology Project (GPCP) Monthly Precipitation Analysis (1979–Present). *J. Hydrometeor.*, **4**, 1147−1167.

Annamalai, H., S. P. Xie, J. P. McCreary, and R. Murtugudde, 2005: Impact of Indian Ocean sea surface temperature on developing El Niño. *J. Climate*, **18**, 302−319.

Ashok, K., Z. Guan, and T. Yamagata, 2001: Impact of the Indian Ocean Dipole on the relationship between the Indian monsoon rainfall and ENSO. *Geophys. Res. Lett.*, **28**, 4499−4502.

Goswami, B. N., 1995: A multiscale interaction model for the origin of the tropospheric QBO. *J. Climate*, **8**, 524−534.

Guan, Z., and T. Yamagata, 2003: The unusual summer of 1994 in East Asia: IOD teleconnections. *Geophys. Res. Lett.*, **30**, 1544−1547.

Izumo, T., J. Vialard, M. Lengaigne, C. B. Montegut, S. K. Behera, J.-J. Luo, S. Cravatte, S. Masson, and T. Yamagata, 2010: Influence of the state of the Indian Ocean Dipole on the following year's El Niño. *Nature Geosci.*, **3**, 168−172.

Ju, J., and J. M. Slingo, 1995: The Asian summer monsoon and ENSO. *Quart. J. Roy. Meteor. Soc.*, **121**, 1133−1168.

Kalnay, E., and co-authors, 1996: The NCEP/NCAR 40-year reanalysis project. *Bull. Amer. Meteor. Soc.*, **77**, 437−472.

Kawamura, R., 1998: A possible mechanism of the Asian summer monsoon-ENSO coupling. *J. Meteor. Soc. Japan*, **76**, 1009−1027.

Loschnigg, J., G. A. Meehl, P. J. Webster, J. M. Arblaster, and G. P. Compo, 2003: The Asian monsoon, the Tropospheric Biennial Oscillation, and the Indian Ocean zonal mode in the NCAR GCM. *J. Climate*, **16**, 1617−1642.

Meehl, G. A., 1987: The annual cycle and interannual variability in the tropical Pacific and Indian Ocean region. *Mon. Wea. Rev.*, **115**, 27−50.

Meehl, G. A., 1993: A coupled air-sea biennial mechanism in the tropical Indian and Pacific regions: Role of the ocean. *J. Climate*, **6**, 31−41.

Meehl, G. A., 1997: The South Asian monsoon and the Tropospheric Biennial Oscillation. *J. Climate*, **10**, 1921−1943.

Meehl, G. A., and J. M. Arblaster, 2001: The Tropospheric Biennial Oscillation and Indian monsoon rainfall. *Geophys. Res. Lett.*, **28**, 1731−1734.

Ogasawara, N., A. Kitoh, T. Yasunari, and A. Noda, 1999: Tropospheric Biennial Oscillation of ENSO-monsoon system in the MRI coupled GCM. *J. Meteor. Soc. Japan*, **77**, 1247−1270.

Pillai, P. A., and K. Mohankumar, 2007: Tropospheric Biennial Oscillation of the Indian summer monsoon with and without the El Niño−Southern Oscillation. *Int. J. Climatol.*, **27**, 2095−2101.

Rasmusson, E. M., and T. H. Carpenter, 1983: The relationship between eastern equatorial Pacific sea surface temperature and rainfall over India and Sri Lanka. *Mon. Wea. Rev.*, **111**, 517−528.

Rayner, N. A., D. E. Parker, E. B. Horton, C. K. Folland, L. V. Alexander, D. P. Rowell, E. C. Kent, and A. Kaplan, 2003: Global analyses of sea surface temperature, sea ice, and night marine air temperature since the late nineteenth century. *J. Geophys. Res.*, **108**, D144407, doi:10.1029/2002JD002670.

Saji, N. H., B. N. Goswami, P. N. Vinayachandran, and T. Yamagata, 1999: A dipole mode in the tropical Indian Ocean. *Nature*, **401**, 360−363.

Sakai, K., R. Kawamura, and Y. Iseri, 2010: ENSO-induced tropical convection variability over the Indian and western Pacific oceans during the northern winter as revealed by a self-organizing map. *J. Geophys. Res.*, **115**, D19125, doi:10.1029/2010JD014415.

Tamura, T., K. Taniguchi, and T. Koike, 2010: Mechanism of upper tropospheric warming around the Tibetan Plateau at the onset phase of the Asian summer monsoon. *J. Geophys. Res.*, **115**, D02106, doi:10.1029/2008JD011678.

Tamura, T., and T. Koike, 2010: Role of convective heating in the seasonal evolution of the Asian summer monsoon. *J. Geophys. Res.*, **115**, D14103, doi:10.1029/2009JD013418.

Tokinaga, H., and Y. Tanimoto, 2004: Seasonal transition of SST anomalies in the tropical Indian Ocean during El Niño and Indian Ocean dipole years. *J. Meteor. Soc. Japan*, **82**, 1007−1018.

Trenberth, K. E., 1975: A quansi-biennial standing wave in the southern hemisphere and interrelations with sea surface temperature. *Quart. J. Roy. Meteor. Soc.*, **101**, 55−74.

Webster, P. J., A. M. Moore, J. P. Loschnigg, and R. R. Leben, 1999: Coupled ocean–atmosphere dynamics in the Indian Ocean during 1997−1998. *Nature*, **401**, 356−360.

Webster, P. J., and S. Yang, 1992: Monsoon and ENSO: Selectively interactive systems. *Quart. J. Roy. Meteor. Soc.*, **118**, 877−926.

Xavier, P., C. Marzin, and B. Goswami, 2007: An objective definition of the Indian summer monsoon season and a new perspective on the ENSO-monsoon relationship. *Quart. J. Roy. Meteor. Soc.*, **133**, 749−764.

Xie, S. P., K. Hu, J. Hafner, H. Tokinaga, Y. Du, G. Huang, and T. Sampe, 2009: Indian Ocean capacitor effect on Indo-western Pacific climate during the summer following El Niño. *J. Climate*, **22**, 730−747.

Yuan, Y., H. Yang, W. Zhou, and C. Li, 2008: Influences of the Indian Ocean dipole on the Asian summer monsoon in the following year. *Int. J. Climatol.*, **28**, 1849−1859.

Manuscript received 2 November 2010, accepted 22 December 2010
SOLA: http://www.jstage.jst.go.jp/browse/sola/